SEIBERSDORF LABORATORIES

ILSC® 2023

Conference Proceedings

Reference information for this proceedings paper

K. Schulmeister, P. Rauter, B.E. Stuck

Review of experimental and computer model retinal injury thresholds in the wavelength regime of 1300 nm to 1400 nm,

International Laser Safety Conference, ILSC 2023, USA, Paper #L0501, pages 79-86

Published by the Laser Institute of America, 2023, Orlando, Florida, USA

REVIEW OF EXPERIMENTAL AND COMPUTER MODEL RETINAL INJURY THRESHOLDS IN THE WAVELENGTH REGIME OF 1300 NM TO 1400 NM

Paper #L0501

Karl Schulmeister[1], Patrick Rauter[1], Bruce E. Stuck[2]

[1]Seibersdorf Laboratories, 2444, Austria
[2]Consulting Biophysicist, San Antonio, TX, USA

Abstract

Experimental and computer-model retinal injury thresholds in the regime of 1300 nm to 1400 nm indicate a need to revise the wavelength dependence of the laser safety exposure limits (MPEs) of ANSI Z136.1-2014, ICNIRP and IEC 60825-1:2014. The wavelength dependence of the MPE is expressed by the factor C_C in ANSI laser safety standard and the ICNIRP laser exposure limit guideline, and C_7 in the IEC laser safety standard; all in the same way. Additionally to the retinal thermal limit, there are limitations provided by dual limits, such as to protect the cornea, that indirectly also limit the energy that passes through the pupil. Experimental injury thresholds in the pulsed regime are available by Vincelette et al. (2009) for a wavelength of 1318 nm in the pulsed regime, as well as by Lund et al. (1981) for 1338 nm mixed with 1318 nm emission. For a relaxed eye of the non-human primate, the exposures in these experiments do not represent small sources but are extended sources (extended retinal images). When the retinal image extent is determined for an actual laser source, a respective C_E factor (C_6 in the IEC standard) is applicable to increase the MPEs. The experimental data show that injury thresholds are very close or are below the MPE when the MPE is calculated for the respective retinal image diameter. Computer model thresholds fit well with the experimental data points. Computer model thresholds are presented in terms of wavelength dependence, pulse duration dependence and retinal image diameter. These can be used to provide input for a discussion to improve the respective MPEs.

General Issues

Wavelength Dependence of MPEs

In 2014, the latest edition of ANSI Z136.1 [1] was published, featuring a substantial increase of the factor C_C of the retinal limits applicable in the wavelength range between 1150 nm and 1400 nm. The same factor was recommended by ICNIRP in the 2013 update of the laser guidelines [2]. IEC 60825-1 [3] uses the symbol C_7 for this factor, with values copied from to the ICNIRP guidelines. In the remainder of this paper, the symbol C_C will be used, but the discussion naturally applies to IEC 60825-1:2014 in the same way, both to the ocular MPEs as well as to the AEL for Class 1 and Class 1M.

The biophysical background of C_C is the pre-retinal absorption, i.e. the absorption of radiation by the media in front of the retina (cornea, aqueous, lens, vitreous) [4, 5]. This absorption reduces the power that arrives at the retina, and in a way protects the retina. Due to the drastic increase of C_C in the 2013/2014 ANSI, ICNIRP and IEC revision, it was necessary to define additional limits to protect the cornea for wavelength range of 1300 nm to 1400 nm. This was done by ANSI, ICNIRP and IEC in different ways, as discussed in our ILSC 2019 paper [6, 7]. Figure 1 shows the AEL for Class 1 (i.e. the ocular MPE multiplied by the area of the 7 mm diameter limiting aperture) for a pulse duration of 1 ms and the angular subtense of the apparent source $\alpha = 1.5$ mrad.

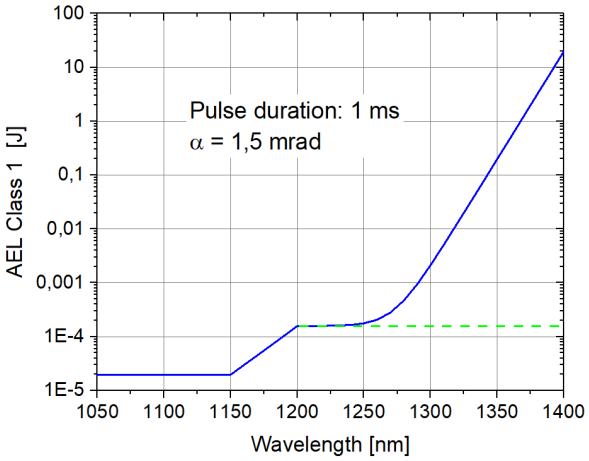

Figure 1 The AEL for Class 1 as function of wavelength. The blue solid line shows the AEL since the 2014 update, the green dashed line shows the earlier AEL.

In Figure 1, the logarithmic increase of C_C for wavelengths above 1250 nm can be seen. From 1050 nm to 1250 nm, there is an increase of a factor of 9, while between 1050 nm and 1400 nm there is an increase of a factor of 1 million.

Transmissivity of Pre-retinal Ocular Media

To compare the computer model data with experimental thresholds obtained with rhesus monkeys, ocular media dimensions and therefore pre-retinal absorption applicable to a young rhesus monkey were used. Such an eye size is comparable to the eye size of a human baby [8-11]. Figure 2 shows calculated spectral transmissivities of the pre-retinal media. The data for the adult human and the young NHP is taken from CIE report 203 [12]. For the human baby, the respective thicknesses were reduced by a factor of 0.78 from the human adult, in order to obtain an axial length of 19 mm. Such an axial length was chosen based on data by Lotmar [11] and Hussain [13] noting that the axial length of the infant eye increases rather rapidly from about 17 mm at birth to 20 mm at 12 months of age, 21 mm at age 4, etc.

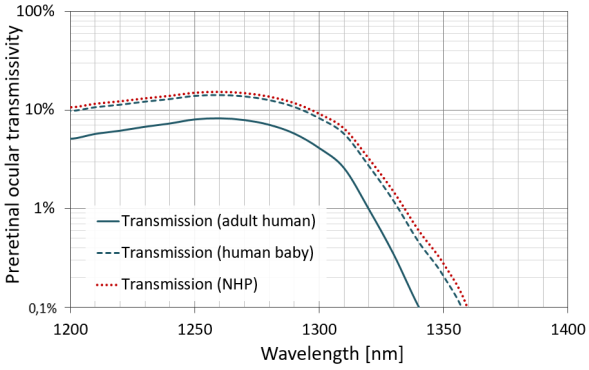

Figure 2 Spectral transmissivity for an adult human and a young rhesus monkey from CIE Report 203. The data for the human baby was obtained by scaling the axial length.

When the retinal injury threshold data (both experimental and from the computer model) is given in terms of power or energy incident on the surface of the eye, a low transmissivity value results in high injury thresholds. Consequently, in the wavelength region of interest, an adult human will have higher injury thresholds as compared to a human baby. Figure 3 shows the ratio of the calculated transmissivity values for the young rhesus monkey vs. the nominal adult human eye. Due the similarity of eye dimensions for human babies with young rhesus monkeys, the data is also approximately representative for human babies vs. human adults. For the wavelength of 1320 nm, the factor is equal to 3.

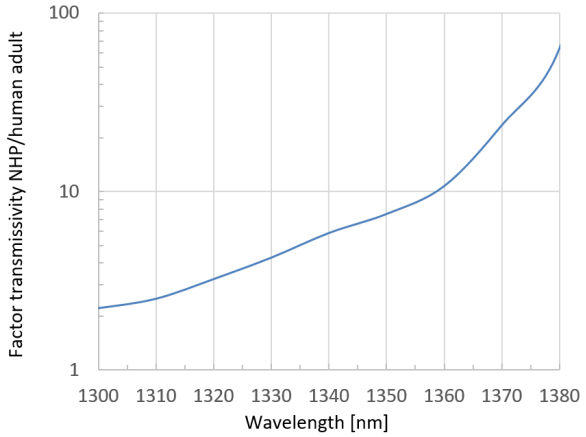

Figure 3 The ratio between the transmissivity of a NHP eye (rhesus monkey) and human adult eye increases with increasing wavelength.

Computer model applicability

We present data from our computer model to predict retinal thermal injury. The model was validated against applicable non-human primate (NHP) ED50 injury thresholds for pulse durations above approximately 100 µs [14], since microcavitation effects are not included in the model.

In the wavelength range above about 1300 nm and exposure durations of the order of 100 ms and above, thermal lensing (also referred to as thermal blooming) leads to an increase of the retinal irradiance profile [15, 16]. For a given intra-ocular power, this reduces the irradiance on the retina and thus increases the injury threshold when expressed as intraocular power. Vincellette [16] noted that for pulse durations longer than 100 ms, it was not possible to damage the retina, since the cornea would be damaged at lower power levels even for relatively large corneal irradiance diameters. She attributed this to the effect of thermal lensing. Our computer model does not include a sub-model for thermal lensing, and consequently pulse durations above 100 ms are not in the scope of this paper.

We will therefore limit the computer model data in this paper to the pulse duration regime of 100 µs to 100 ms.

Since there is some uncertainty about the retinal irradiance profile for the nominal case of $\alpha = 1.5$ mrad, this was not included in the present discussion.

Due to large uncertainties for the pre-retinal transmissivity for wavelengths approaching 1400 nm, we limit the modelling range to wavelengths up to 1360 nm.

Experimental Data

For the wavelength range and pulse duration regime of relevance for a comparison with model predictions, there is a paucity in experimental threshold data for rhesus monkeys. Table 1 lists two relevant rhesus monkey studies that we have identified [5, 17]. Data from experimental threshold studies with rabbits [18] were not included. We also did not include an experimental study for 300 µs pulse duration and 1315 nm wavelength with rhesus monkeys, where the endpoint was observation shortly after the exposure and the beam properties where not sufficiently described so that it was difficult to calculate the expected retinal image diameter [19].

The endpoint of the study by Lund et al. was 1 hour observation after exposure, while it was 24 hours for the study by Vincelette et al.. Exposure sites were paramacular for the Lund study and macular for the Vincelette study. As part of the project with first author Vincelette, an additional experiment was conducted with a +2.1 D lens intended to compensate for chromatic aberration [20]. From the beam parameter information available, the retinal image diameter was calculated with the ABCD technique and a Le Grand schematic eye for a relaxed eye with focal length 13.35 mm (74.0 D) at a wavelength of 590 nm. Chromatic aberration (i.e. the wavelength dependence of the refractive index) was included in the calculations, resulting in a predicted retinal irradiance diameter of 178 µm for the Lund et al. study and 213 µm for the Vincelette et al. study without the lens, respectively. For the additional experiment with the added lens, we calculated a retinal image diameter of 156 µm, which is consistent with the divergence of the beam.

Table 1. Characteristic properties of the lasers used in two experimental studies. The retinal image diameter was calculated based on the beam properties as described in the respective publications.

Source	Wavelength [nm]	Pulse duration [ms]	Divergence [mrad]	Retinal image diameter [µm]
Lund, 1981	40% @ 1318 60% @ 1338	0.65	2.3 mrad (1/e)	178 (1/e)
Vincelette, 2009	1318	80	13.3 mrad ($1/e^2$)	213 (1/e)
With +2.1 D lens				156 (1/e)

Table 2. Experimental threshold data for rhesus monkeys in the pulsed regime. *R* is the ratio of the computer model predictions to the experimental ED50.

Source	ED50 [J]	*R*	AEL Class 1 Human adult [J]	AEL/ED50
Lund, 1981	0.36	0.98	0.43	1.2
Vincelette, 2009	1.16	0.62	2.34	2.0
With +2.1 D lens	0.89	0.59	1.72	2.0

Experimental ED50 data and AELs for Class 1 are shown in Table 2. With the input data summarized in Table 1, our computer model predicts injury thresholds that fit well with the experimental ED50: the prediction for the wavelength-mixed study by Lund et al. is basically identical with the ED50, and the model prediction is a factor 0.62 of the ED50 for the Vincelette et al. study; in other words, the computer model prediction is a factor 1.6 below the ED50. Considering a number of sources of potential uncertainties in the model as well as in the experimental studies, this can be characterized as to be a good fit. Consequently, the computer model, with due consideration of uncertainties. can be considered as sufficiently validated (see also [14]) to provide valid trends of injury thresholds as function of wavelength, pulse duration and retinal image diameter.

Table 2 also lists the AEL for Class 1 where α was derived for the air-filled nominal human adult eye (17 mm), i.e. dividing the retinal image diameter by 17 mm to obtain α. Compared to using the nominal size (distance of lens system to retina in an air-filled eye) for a human baby of less than 17 mm, this is a non-conservative choice, resulting in a higher AEL for the comparison with the respective ED50. For the Lund et al. study, the combination of wavelengths was accounted for by a combined value of C_C. The table shows that the AEL is *above* the experimental ED50, i.e. permits higher exposure than the injury threshold for the rhesus monkey. For the data by Vincelette, the AEL is a factor of 2 above the ED50, for the data by Lund by a factor of 1.2. This already indicates that at least for a human baby, with a pre-retinal transmissivity comparable to that of the rhesus monkey, the MPE and therefore the AEL for Class 1 might be too high, at least in the pulsed regime investigated.

In order to gain a better understanding which parameter is relevant for the mismatch between MPE and ED50, thresholds as function of wavelength, pulse duration and retinal image diameter were calculated for a nominal adult human eye, as presented in the next section. The study can be complemented at a later date by modelling of smaller human eyes.

Comparison of Model Threshold with MPEs

Comment on the choice of angular subtense

For an emmetropic eye, in the visible wavelength range, accommodation to infinity means that the focal length of the eye is equal to the lens-retina distance. That is, for accommodation to infinity in the visible wavelength range, the retina is located in the focal plane of the eye's lens system. In this case, the angular subtense of the retinal image is equal to the divergence of the beam.

For the wavelength range under consideration in this paper, the optical power of the eye is smaller than in the visible wavelength range, which is referred to chromatic aberration. When the eye is accommodated to infinity in the visible wavelength range, for the wavelength range under discussion, the beam waist will be located somewhat behind the retina, resulting in a larger retinal image. A task-oriented awake human can accommodate to distances closer than infinity, compensating for chromatic aberration and reducing the retinal image diameter for the case of a well-collimated beam.

In the general case, a certain laser beam and a certain accommodation of the eye will result in a corresponding retinal image irradiance profile. The angular subtense of the apparent source α characterizes the retinal image diameter and is a parameter which determines the MPE. When the retinal image diameter D_{ret} is given (such as from simulations), a certain distance of the lens system to the retina L_{eye} - usually given for an equivalent air-filled eye - needs to be assumed to determine α:

$$\alpha = \frac{D_{ret}}{L_{eye}} \qquad (1)$$

For the nominal human adult eye, the distance for an air-filled eye L_{eye} = 17 mm, while for the nominal rhesus monkey eye, L_{eye} = 13.4 mm. The relationship can also be seen from the starting point of a given laser beam where a small eye and a larger eye accommodate to a given location in the beam, as the "apparent source". While the angle α that characterizes the angular subtense of the retinal image (assuming that the pupil has the same diameter or does not influence the retinal image) is the same for both eyes, the retinal image for the smaller eye will be smaller than compared to the larger eye. Thus, a smaller eye can be assumed to be associated to lower thresholds (expressed as intraocular energy) not only because of the higher transmittance in the wavelength range under discussion, but also because of the potentially smaller retinal image. One option, when exposure of human babies are an issue, would be to reduce the retinal image for the determination of the MPE and the AEL of Class 1, or to introduce a correction factor. The simplified nominal difference of the image diameter can be characterized by the ratios of L_{eye}. For the comparison with rhesus monkey eyes, the ratio would be 17 mm/ 13.4 mm = 1.26. This can be expected as to be the approximate difference in thresholds (for the same transmissivity) in the regime where the dependence of the threshold goes linear with α. The theoretical difference in the regime of the retinal image being larger than α_{max} goes with the square of the ratio, i.e. 1.6. This issue of potentially smaller retinal image applies additionally to the higher pre-retinal transmissivities for small eyes.

For the ANSI Z136.1 standard, with the main scope of the safe use of professional high-power lasers, the potential exposure of human baby eyes is less of a concern. However, for the ICNIRP guidelines and the IEC 60825-1 Class 1 limits, the whole population is of relevance.

In this paper, we discuss the computer model results for a human adult eye. The issue of smaller eyes can be the topic of further studies.

When ray tracing or measurements with an imaging lens and an array detector show that for a given beam and a given accommodation state of the eye, the retinal image is of a given diameter, then for product safety classification based on IEC 60825-1 (but also potentially for an MPE analysis based on the ANSI standard) the respective value of $C_E > 1$ will be used to determine the AEL and the MPE. A critical review of the MPEs, for the case of an extended source, needs to be based on the respective value of $C_E > 1$. It does not appear justified to compare injury thresholds obtained with extended retinal images with an MPE determined for $C_E = 1$, as was for instance done in the discussion found in reference [20]. We argue that a sufficient safety margin should also exist when the retinal irradiance profile is determined for a given exposure or laser emission and the MPE or the AEL for Class 1 is based on the respective determined retinal irradiance profile.

General information on presented data

In the following, we compare computer model thresholds with the respective MPEs. The MPEs are represented by intraocular energy values, i.e. obtained by multiplying the MPE by the area of a 7 mm limiting aperture. This is also referred to as AEL for Class 1. The limits are the same in ANSI and in the IEC standard. The retinal irradiance profile is assumed to be circular and homogeneous, referred to as top-hat profile. The injury thresholds are calculated for a NHP eye in terms of transmissivity so that the data is also representative of the optical path length of human baby eyes. For a given value of α, the retinal image diameter was, however, calculated with a nominal human adult eye via multiplication of α with 17 mm air-equivalent distance between the imaging system of the eye and the retina. The computer model as optimized for macular exposures was used.

In the following subsections, the "safety margin" will be plotted, i.e. the ratio obtained by dividing the computer model threshold by the MPE. When this ratio is less than one, the predicted injury threshold is below the MPE (and therefore lower than the AEL for Class 1), indicating the need to lower the MPEs to provide sufficient protection. The discussion and presentation is based on intra-ocular energy. Therefore, when the beam diameter at the eye is larger than the pupil, the energy within the laser beam is permitted to be higher than the threshold.

The t-dependence of α_{max} has been considered by increasing the MPE with α^2 for angular subtense values exceeding α_{max} (which can be referred to an adjustment of the MPE for an open measurement field of view, see discussion in reference [21]).

Dependence on Wavelength

Figure 4 shows the threshold/MPE ratio as function of wavelength for pulse durations t between 100 µs and 100 ms. Figure 4a shows the data for α = 5 mrad; the ratio obtained for 10 mrad and 20 mrad is similar. Figure 4b shows the data for α = 100 mrad; the ratio obtained for 40 mrad and 70 mrad is similar.

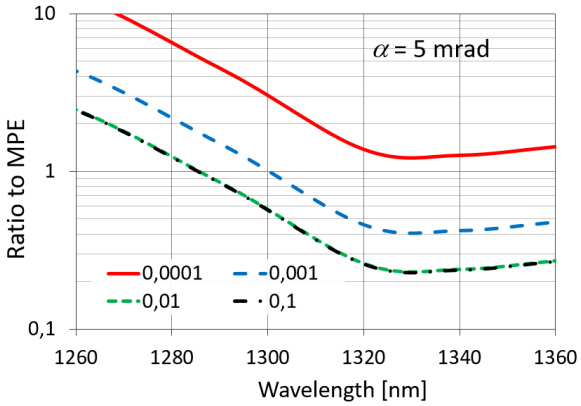

Figure 4a. The threshold/MPE ratio as function of wavelength for four selected pulse durations given in the legend in seconds, and α = 5 mrad.

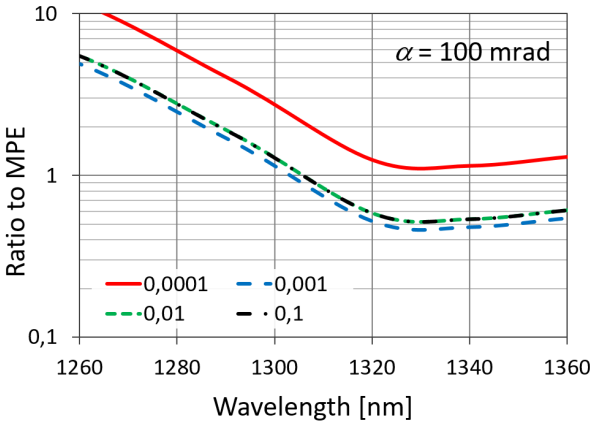

Figure 4b. As for Figure 4a, but for α =100 mrad.

The general trend of the ratio curves is that there is a sufficient safety margin for the wavelength of 1260 nm. The safety margin then steadily decreases and for pulse durations of 1 ms and longer becomes less than 1 for wavelengths above about 1300 nm. The minimum is reached at about 1330 nm.

It can be seen that for both values of α, the curve for t = 100 µs lies above 1. However, the lowest point, found at a wavelength of about 1330 nm, is only a factor of 1.3 above 1. Considering the uncertainty of the computer model and that infant humans with smaller eyes will have a higher transmissivity and lower threshold expressed as intra-ocular energy, this safety margin does not appear to be sufficient. The threshold/MPE ratios for pulse durations of 1 ms, 10 ms and 100 ms are well below a value of 1: in the range of 0.5 for α = 100 mrad and only about 0.2 for α = 5 mrad for 10 ms and 100 ms pulse duration. That is, the MPE permits intraocular energies that are 5

times the predicted injury threshold for the adult human eye.

Dependence on Exposure Duration

Figure 5 shows the threshold-MPE ratio as function of exposure duration, for the selected wavelengths of 1250 nm and 1320 nm. Figure 5a is for $\alpha = 5$ mrad and Figure 5b is for $\alpha = 100$ mrad.

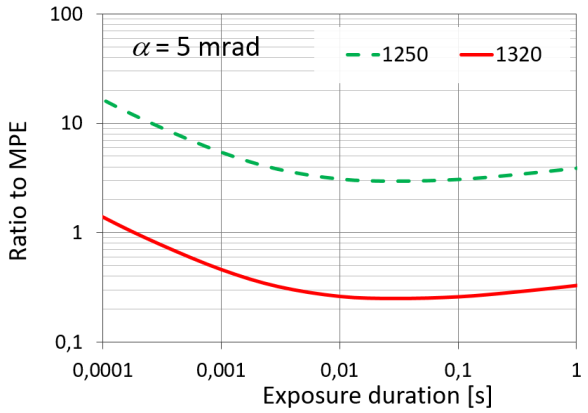

Figure 5a. The threshold/MPE ratio for two selected wavelengths given in the legend in nanometer, and $\alpha =$ 5 mrad.

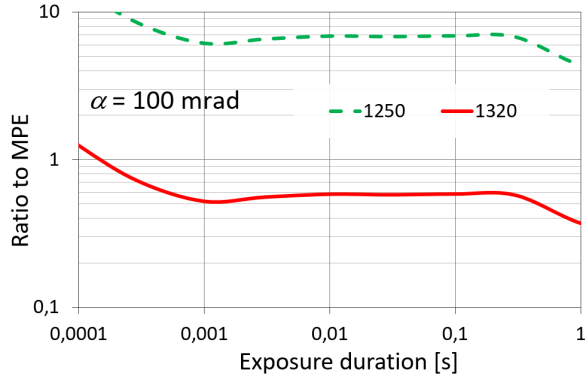

Figure 5b. As for Figure 5a, but for $\alpha = 100$ mrad.

For the 100 mrad data, the ratio is constant between 1 ms and more than 100 ms. This means that the basic trend of the MPE as function of pulse duration is consistent with the *t*-dependence of the injury thresholds. However, the ratio for 1320 nm is at a level of 0.6, i.e. the MPE is almost a factor of 2 above the predicted injury threshold. For $\alpha = 5$ mrad, the ratio is not as constant as for the case of 100 mrad, but also does not vary drastically between the pulse duration of 1 ms and 1 second; and for a wavelength of 1320 nm is again considerably less than 1.

Comparison with additional limits

We see above in Figure 4 that there is an apparent mismatch between the wavelength dependence of the MPE and the predicted injury threshold for the adult human eye. This mismatch can be seen in the following Figure 6 for the example of $\alpha = 5$ mrad. Figure 6a is for a pulse duration of 1 ms and Figure 6b is for a pulse duration of 10 ms. Also shown are the permitted intraocular energy levels, derived from limits other than the retinal thermal MPE. These limits are discussed in detail in our ILSC 2019 paper [6]. IEC 60825-1 specifies the Class 3B AEL as dual limit in the wavelength range of interest. In the pulse duration range between 1 ns and 250 ms, the Class 3B limit is a constant value of 150 mJ. Also shown is the ANSI limit to protect the cornea. The limiting aperture in the pulsed regime has a diameter of 1 mm. Multiplication of the limit which is given as corneal radiant exposure by the area of the limiting aperture results in the energy that is permitted to pass through a 1 mm aperture. When the beam diameter at the cornea is larger than 1 mm, a correspondingly larger level is permitted in the beam, that could theoretically also pass through a correspondingly large pupil. The level permitted by the corneal limit, for the case of a 7 mm beam diameter at the cornea is also shown. The strong wavelength dependence of the ANSI limit to protect the cornea can be seen. Additionally, the MPE for the skin is shown, also transformed into permitted energy levels based on a 1 mm limiting aperture. This limit is defined in amendment A11:2021 to EN 60825-1:2014 to protect the cornea [22], since it was found that the Class 3B limit for wavelengths approaching 1400 nm does not sufficiently protect the cornea [6,7].

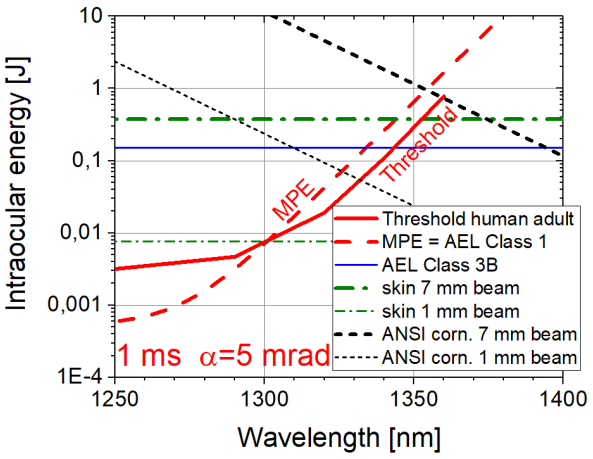

Figure 6a. The retinal thermal MPE and the predicted injury threshold plotted as function of wavelength. The permitted levels derived from dual limits are also shown. The pulse duration equals 1 ms.

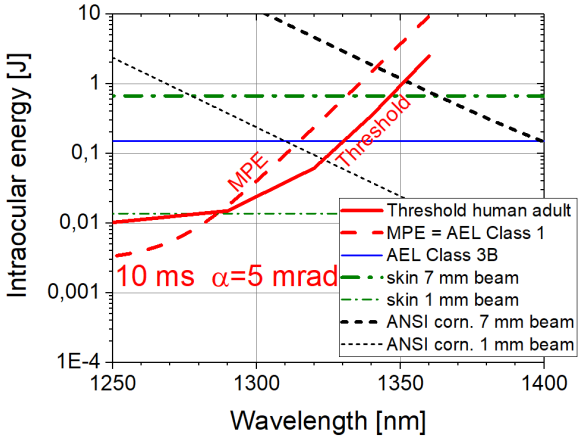

Figure 6b. As Figure 6a, but for a pulse duration of 10 ms.

As could also be seen from figures in earlier sections, the predicted injury threshold is significantly below the MPE for wavelengths in the regime of wavelengths roughly above 1300 nm. The dual limits do not sufficiently limit the permitted intra - ocular energy, with the exception of the skin MPE and beam diameters of 1 mm or less. For the case of larger beam diameters, the skin MPE is also not sufficiently limiting the permitted intra - ocular energy. This is also the case for the Class 3B limit. The ANSI corneal limit only protects for beam diameters of 1 mm and wavelengths above about 1330 nm.

The retinal threshold and MPE is plotted here for α = 5 mrad. Larger values of α are associated with both larger MPEs and larger injury thresholds, so that the AEL for Class 3B at some point becomes lower than the MPE and affords protection for the retina. At which level of α this is the case depends on the pulse duration. For instance, for t = 80 ms in the Vincelette et al. study [5] shown in Table 2, the reported ED50 was above the Class 3B AEL of 150 mJ.

Summary and Conclusions

Experimental ED50 data obtained with rhesus monkeys are presented and found to be below the respective MPE, when the MPE is determined based on the extended nature of the retinal irradiance profile. The pre-retinal transmission of rhesus monkey eyes can be assumed to be equivalent to human babies.

Computer model predictions for adult human eyes, for the pulse duration range of 100 µs to 100 ms show that the wavelength dependence of the MPE does not follow predicted injury threshold. In the regime above about 1300 nm, the MPE appears to be too high. For the worst case found (α = 5 mrad, pulse duration between 10 ms and 100 ms, wavelength range 1315 nm to 1360 nm), the ratio between thresholds and MPEs was less than 0.3. In other words, the MPE permitted exposure levels that exceed the predicted threshold for human adults by more than a factor of 3.

Compared to the eye of a human baby, the human adult eye in the wavelength range under consideration has lower transmissivity. For the wavelength of 1315 nm this can be assumed to be roughly a factor of 3 (depending on the size of the eyes). Additionally, for a given value of angular subtense of the apparent source and the retinal image α, a smaller eye can be assumed to have a smaller retinal image diameter. Both issues raise additional concerns for laser products used as consumer products. It appears prudent to question if the increase of C_C of the 2014 update of the ANSI Z136.1 and IEC 60825-1 standards were justified in all cases, particularly when the extended nature of the retinal irradiance profile is used for the determination of the MPE and the AEL of Class 1.

It should be kept in mind that neither ANSI Z136.1 nor IEC 60825-1 require to use C_E = 1 (C_6 =1) for collimated beams in the respective wavelength range. It is permitted to determine the MPE and AEL for Class 1 with the respective extended source when determined for a given accommodation of the eye. The IEC standard specifically requires the variation of the accommodation in the classification process. For a well collimated laser beam in the respective wavelength range, accommodation to a location shorter than infinity will compensate for chromatic aberration, resulting in a correspondingly small retinal image. However, some laser products are associated to extended sources for all accommodation states, such as line lasers, DOE projectors or scanned laser emission. A manufacturer has the option to classify the product as extended source and the applicable MPEs and AEL need to also be appropriate for extended sources.

Since for an amendment of the limits, several factors need to be considered and studied further, we do not discuss in this paper in what way the MPEs could be updated.

Acknowledgements

We greatly appreciate frequent discussions with and valuable support by David Jack Lund †.

We thank Mathieu Jean (now at ZKW Austria) for literature research, data analysis and plotting of data for Figure 1 and Figure 2.

References

[1] American National Standards institute (2014), American National Standard for the safe use of Lasers, Z136.1-2014, Laser Institute of America, Orlando FL.

[2] ICNIRP (2013), ICNIRP Guidelines on limits of exposure to laser radiation of wavelengths between 180 nm and 1000 µm, Health Physics 105, 271 - 295.

[3] International Electrotechnical Commission (2014), IEC 60825-1 Safety of laser products – Part 1: Equipment classification and requirements, Ed 3.0, IEC, Geneva, 2014.

[4] Zuclich J.A., Lund D.J., Stuck B.E. (2007), Wavelength dependence of ocular damage thresholds in the near-IR to far-IR transition region: proposed revision to MPEs, Health Physics 92, 15 - 23.

[5] Vincelette R.L., Rockwell B.A., Oliver J.W. et al. (2009), Trends in retinal damage thresholds from 100-millisecond near-infrared laser radiation exposures, Laser Surg. Med. 41, 382 - 390.

[6] Schulmeister K., Jean M., Lund D.J., Stuck B.E. (2019), Comparison of laser induced corneal injury thresholds with safety limits, ILSC 2019 Conference Proceedings, Paper #303, 102 - 110.

[7] Schulmeister K., Jean M., Stuck B.E. (2023), Comparison of laser induced corneal injury thresholds with safety limits, to be submitted to J. Laser Appl. 2023.

[8] Smith D.A. and Smith G. (2002), Optics of the human eye, Butterworth-Heinemann.

[9] Qiao-Grider Y., Hung L.F., Kee C. et al. (2007), Normal ocular development in young rhesus monkeys (Macaca mulatta), Vision Res. 47, 1424 - 1444.

[10] Hainline L., Riddell P. et al. (1992), Development of accommodation and convergence in infancy, Behav. Brain Res. 49, 33 - 50.

[11] Lotmar A. (1976), Theoretical model for the eye of new-born infants, Albrecht von Graefes Archiv für klinische und experimentelle Ophthalmologie, Vol. 198, 179 - 185.

[12] CIE (2012), A computerized approach to transmission and absorption characteristics of the human eye, Technical Report CIE 203:2012, CIE Vienna.

[13] Hussain R.N., Sahid F., Woodruff G. (2014), Axial length in apparently normal pediatric eyes, Eur J Ophthalmol 24, 120-123.

[14] Jean M. and Schulmeister K. (2017), Validation of a computer model to predict laser induced retinal injury thresholds, J. Laser Appl. 029, 032004.

[15] Vincelette R.L., Oliver J.W., et al. (2009), Thermal lensing from near-infrared laser radiation in an artificial eye. Proc. of SPIE, San Jose, CA, SPIE 7175.

[16] Vincelette R.L. (2009), Thermal lensing in ocular media, PhD Thesis University of Texas at Austin.

[17] Lund D.J., Stuck B.E., and Beatrice E.S. (1981), Biological research in support of project MILES, Report No. 96, Letterman Army Institute of Research, San Francisco, CA.

[18] Jiao L. et al. (2019), Retinal damage thresholds from 100-millisecond laser radiation exposure at 1319 nm: a comparative study for rabbits with different ocular axial lengths; Biomed Opt Expr #354510.

[19] Zuclich J.A. et al. (2001), High-power lasers in the 1.3-1.4 µm wavelength range: ocular effects and safety standard implications, SPIE Proceeding Vol. 4246, 78-88.

[20] Rockwell B. (2019), private communication.

[21] Schulmeister K., Sliney D.H., Stuck B.E. (2018), Comments on the application of the ICNIRP laser exposure limits, in: Proceedings of NIR 2018 Dresden, Ed.: Reidenbach HD, Brose M and Joosten St; TÜV Media GmbH, Köln; pages 321 - 345.

[22] Schulmeister K. (2022), The European Amendment A11:2021 to EN 60825-1, White Paper, Seibersdorf Laboratories.

[23] Henderson R. and Schulmeister K. (2004), Laser Safety, Taylor & Francis Group, New York, London.

[24] Schulmeister K. (2005), The Apparent Source' – A Multiple Misnomer, Proceedings ILSC 2005 Conference Proceedings, Laser Institute of America, p. 91-98.

[25] Schulmeister K (2015), Classification of extended source products according to IEC 60825-1, ILSC 2015 Conference Proceedings Paper #C101, Page 271-280.

Almost all the publications of the Seibersdorf Laboratories team can be downloaded from:

https://laser-led-lamp-safety.seibersdorf-laboratories.at/downloads